

Computational Fluid Dynamics Study of Optimized Hypersonic Leading Edge Geometries

W. Schuyler Hinman* Simon Schmitt† Craig T. Johansen ‡

University of Calgary, Calgary, Alberta, T2N 1N4, Canada

Patrick E. Rodi§

Lockheed Martin Corporation, Houston, TX 77258-8487

An aerothermal optimization study of two-dimensional hypersonic leading edge geometries has been performed. The accuracy of a simplified model and a reduced order numerical model was assessed through comparison to simulations of the compressible Navier-Stokes equations performed in OpenFOAM. Specifically, the estimated surface pressure, and laminar convective heating distributions have been compared. The simplified model was found to have compromised accuracy in regions of high and low surface curvature. The reduced order numerical model was found to give accurate results with significantly reduced computational cost compared to complete Navier-Stokes simulations. Optimizations were then performed using the simplified analysis technique, and the reduced order numerical model. The performance of the optimized hypersonic leading edge geometries was analyzed using OpenFOAM. The results show that both methods achieve a similar geometric result. However, the quality of the optimization is improved by using the reduced order numerical model. An analysis was performed in the design space immediately surrounding the optimized geometry to assess the impact of small geometric changes on aerothermal performance. The results show that even small changes in leading edge geometry can have a significant influence on aerothermal performance.

Nomenclature

$a_1 \dots a_n$	NASA polynomial coefficients
C	Sutherland's constant
C_1, C_2, C_3	Empirical constants for Kays laminar heating method
C_p	Coefficient of pressure
$C_{p,max}$	Stagnation point coefficient of pressure
c_p	Constant pressure specific heat capacity ($J/kg \cdot K$)
c_v	Constant volume specific heat capacity ($J/kg \cdot K$)
H	Total enthalpy (J/kg), Leading edge height (m)
P	Pressure, (Pa)
q_∞	Free-stream dynamic pressure (Pa)
q''	Wall heat-flux (W/m^2)
U	Velocity magnitude (m/s)
R	Axi-symmetric body radius (m)
R_g	Gas constant ($J/(kg \cdot K)$)
r	Radius of curvature (m)
S	Entropy (J/K)
St	Stanton number

*PhD Student, Department of Mechanical Engineering, AIAA Student Member

†Undergraduate research assistant, Department of Mechanical Engineering

‡Assistant Professor, Department of Mechanical Engineering, AIAA Member

§Lockheed Martin Fellow, AIAA Associate Fellow

T	Temperature (K)
θ	Flow deflection angle ($^{\circ}$)
κ	Thermal conductivity ($W/(m \cdot K)$)
μ	Viscosity ($N \cdot s/m^2$)
μ_o	Sutherland's reference viscosity ($N \cdot s/m^2$)
ρ	Density (kg/m^3)
ϕ	Angular leading edge coordinate ($^{\circ}$)

Subscript

aw	Adiabatic wall properties
e	Boundary layer edge properties
w	Wall properties
∞	Free-stream properties

I. Introduction

High lift-to-drag ratio (L/D) supersonic and hypersonic bodies are designed to have sharp leading edges in order to minimize drag.^{1,2} However, sharp leading edges are limited by both manufacturability and by excessive convective heating loads at high Mach number.^{1,2} It is known that heating can be reduced by increasing the bluntness of the leading edge as stagnation point heating obeys an inverse relationship with the square of the local body radius at the stagnation point.³ However, it is a concern for the designers of high speed flight vehicles such as waveriders that blunt leading edge effects could adversely affect the aerodynamic performance of the vehicle. Vehicle drag is increased by the detached bow shock induced by a blunt leading edge. Additionally, the shape of the blunt leading edge alters the stream-wise pressure gradient and therefore can adversely impact the stability of the laminar boundary layer. Drag and heating reduction associated with a laminar flow design can be significant. Design studies have been performed regarding finite leading edge geometries using power law curves⁴ and Bezier curves.^{1,5} The accuracy of using simplified methods to assess the performance of these geometries is not well understood.

In recent work, genetic algorithm (GA) and particle swarm optimization (PSO) was used to optimize a leading edge for heat transfer and pressure drag reduction.^{1,5} Bezier curves were utilized due to the increased geometric flexibility available compared to power-law based geometries. The study by Rodi¹ produced an optimized shape resulting in a decrease in laminar convective heating of 23.4 % and an increase in pressure drag of 17.1 % for the hypersonic laminar conditions investigated. The optimization utilized simplified analysis techniques for the prediction of drag and convective heating. It is of interest to investigate the effect of using simplified analysis techniques on the optimization.

In general, the effectiveness of any optimization routine is limited by the accuracy of its model. An optimization routine executed up to a high precision could still have a less than desirable accuracy. The design space being explored must reflect the region where the analysis technique is sufficiently accurate. Failure to do so could result in non-physical or artificial minima. Additionally, within an appropriate design space, due to reduced accuracy in response to geometric changes, the location of local and global minima may change. Consequently, this question is a major focus of the present work. Do the locations of the minima change due to an increase in physical accuracy?

In the present work, applications of a simplified analysis technique, numerical solutions to the Euler equations plus the boundary layer equations, and simulations of the compressible Navier-Stokes equations are compared. In general, Computational Fluid Dynamics (CFD) simulations of the compressible Navier-Stokes Equations offers the most robust and accurate means of studying a high speed flow problem numerically. Currently, this approach is expensive with regard to both time and computer resources. The expensive nature of the Navier-Stokes equations makes them unsuitable for optimizations with a relatively large and/or complicated design space. For this reason simplified analysis techniques such as the modified Newton's method are employed. In many cases a compromise can be made between the speed of highly simplified analysis techniques and solutions to the Navier-Stokes equations. Herein, a code used for analyzing blunt body flows at the University of Calgary (HyPE2D) is used as an intermediate fidelity analysis tool. The accuracy from three different analysis techniques are compared for a few representative leading edge geometries. An optimization is performed with both the simplified analysis technique (referred to, from here on, as the Newton-Kays model) and HyPE2D. The aerothermal performance of the optimized geometries is

analyzed using rhoCentralFOAM (regarded as the benchmark for accuracy in this study) and compared to the lower fidelity models.

II. Performance Analysis Details

A. Simplified Analysis Details (Newton-Kays Model)

The fastest analysis technique used here is a combination of a simple model for the inviscid external flow, and an integral approach to the laminar boundary layer heat transfer. These are typical engineering style approaches that are highly useful early in a design process but are often supplanted by more sophisticated techniques when more accurate results are required.

A.1. Modified Newton's Method

The modified Newton's method is a simple analytical tool based on the body inclination angle and a prediction of the maximum pressure coefficient in the shock-layer.³ The calculation is given in Equations 1 and 2.

$$C_p = C_{p,max} \sin^2 \theta \quad (1)$$

where:

$$C_p = \frac{p - p_\infty}{0.5 \rho U_\infty^2} \quad (2)$$

Here, $C_{p,max} = 1.8316$ is found using the normal shock relations to calculate the stagnation pressure behind the fore-body shock assuming constant specific heats. The flow deflection angle θ is the difference between the body surface inclination angle and the angle of the oncoming free-stream flow. Once the pressure distribution along the surface is known, the other flow parameters (T , U , ρ) along the body are calculated using the isentropic flow relations.

A.2. Kays Laminar Heating Method

Once the inviscid flow properties are known, the Kays laminar heating method⁶ is used to calculate the distribution of the Stanton number (St) around the leading edge. The calculation is given in Equation 3.

$$St = \frac{C_1 \mu^{0.5} R G_e^{C_2}}{\left(\int_0^x G_e^{C_3} R^2 dx \right)^{0.5}} \left(\frac{T_s}{T_e} \right)^{-0.08} \left(\frac{T_{aw}}{T_e} \right)^{-0.04} \quad (3)$$

Here, $G_e = \rho u_e$, μ is the viscosity (evaluated at film temperature), and C_1 , C_2 , and C_3 are empirical constants. R is the axisymmetric body radius and cancels out of the equation in the two-dimensional case as in this study.

B. HyPE2D Simulation Details

Fast and accurate design tools offer significant advantages over both highly simplified approaches and high quality CFD when applied to optimization design problems. Simplified approximations typically suffer from decreased accuracy, whereas CFD suffers from high computational cost. HyPE2D is a fast and accurate simulation tool for solving two dimensional hypersonic flow over blunt bodies. HyPE2D was developed using the shock-fitting principles outlined by Salas⁷ and the boundary layer modelling described by Schetz.⁸ The solution in the present work is solved assuming that there is no significant viscous-inviscid interaction. However, a correction for viscous-inviscid interactions is easily applicable for low Reynolds number cases as has been performed in a related study pertaining to the expanding flow on the aft-body of a circular cylinder.⁹ In the present formulation, a result for the flow-field is achieved on a personal computer in approximately 100 seconds. The speed of the solution can be increased or decreased by increasing the resolution of the computational grids. The grid resolutions used to solve the Euler equations, and the boundary layer equations, in the genetic algorithm were selected to balance accuracy and computational time. Sufficient accuracy is required to correctly guide the optimization, but fast enough solution time is necessary for the process to remain feasible. The working grids were used in the comparison shown in Section III and gave adequate results, as well as an acceptable solution time.

B.1. Inviscid Flow (Euler Equations)

HyPE2D solves the inviscid flow using the shock-fitting principles outlined in the textbook by Salas.⁷ A finite difference grid is generated between the leading-edge body and an empirically estimated initial bow shock-wave location. The grid is then transformed to a rectangular grid through a coordinate system transformation. A typical grid is shown in Figure 1 for a geometry from Rodi.¹ The unsteady Euler

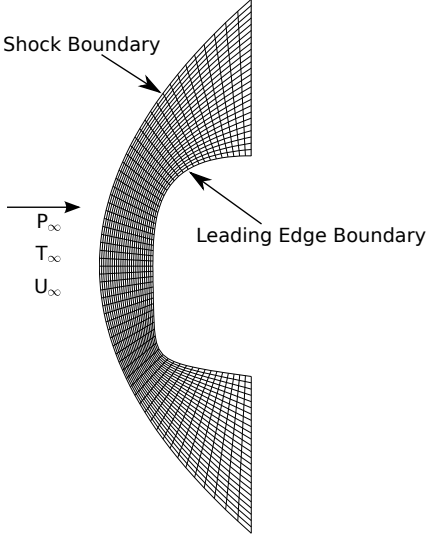


Figure 1. Typical HyPE2D Shock-Fitted Grid

equations are solved on the grid using the MacCormack method.^{3,7} At each step forward in pseudo-time, the location of the shock and the flow properties behind it are updated. The solution is progressed until the field is converged to an acceptable level (wall temperature distribution converged to $1 \times 10^{-3}\%$). Equilibrium properties are recalculated at each time-step using the thermo-physical models outlined in Section D, and are used to calculate the jumps across the shock boundary. The shock-wave is solved numerically using the shock-jump conservation equations. The solution for these equations is achieved iteratively using the Newton-Raphson method for solving non-linear systems of equations.

B.2. Viscous Flow (Boundary Layer Equations)

The viscous flow is solved numerically using the approach outlined by Schetz for solving non-similar compressible boundary layers.⁸ The location of the stagnation point, as well as the properties along the body are taken from the inviscid flow model described in Section B.1. The initial velocity and enthalpy profiles are calculated at the stagnation point using the similarity solution outlined by Cohen and Reshotko.¹⁰ The solution is then marched forward in the stream-wise direction away from the stagnation point along the upper and lower surface of the leading edge using a semi-implicit Crank-Nicholson method. The gas specific heats (c_p , c_v), viscosity (μ), and thermal conductivity (κ) are calculated at each stream-wise step using the models in Section D.

C. OpenFOAM Simulation Details

C.1. Compressible Flow Solver

Two-dimensional Navier-Stokes simulations were performed using the open-source software, OpenFOAM.¹¹ Specifically, the high speed flow solver rhoCentralFoam was used in the simulation. The solver rhoCentralFoam is a density based solver of the unsteady, compressible Navier-Stokes equations.¹² RhoCentralFoam has been shown to give close agreement to experimental data for similar high-speed flows.^{13,14}

C.2. Geometry and Boundary Conditions

The flow-field around each Bezier Curve Leading Edge (BCLE) was meshed using the OpenFOAM native meshing software, blockMesh. A schematic of the domain geometry and boundary conditions are shown in Figure 2. The domain was generated in such a way so as to allow mesh clustering near the shock wave, and clustering of cells in the boundary layer. The outlet boundary on the lower surface of the leading edge was generated on an angle to ensure adequate orthogonality of the cells along the leading edge surface. Grid convergence was checked for the rhoCentralFoam simulations using Richardson extrapolation for peak heat flux, and integrated heat flux. The refined grids typically resulted in less than 2% error in integral heat flux, and less than 5% error in peak convective heat flux, from the Richardson extrapolation prediction.

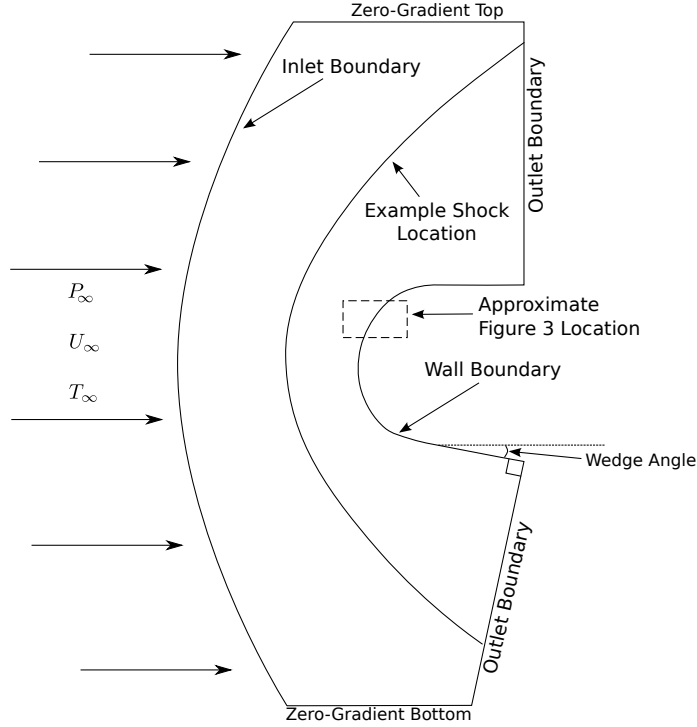


Figure 2. Schematic of OpenFOAM simulation geometry

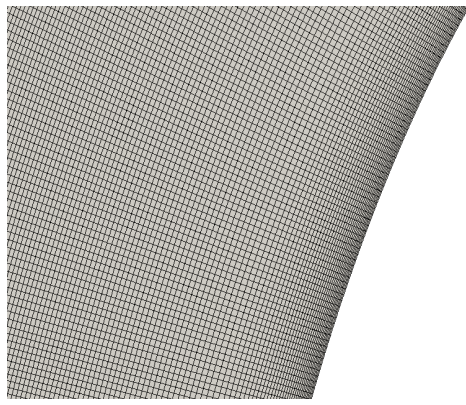


Figure 3. Typical mesh close to wall (see Figure 2 for location)

The simulation inlet conditions are specified with free-stream static pressure ($p_\infty = 1365.78 \text{ Pa}$), static temperature ($T_\infty = 225.636 \text{ K}$), and velocity ($U_\infty = 3014 \text{ m/s}$). These inlet conditions correspond to a Mach number of $M = 10$, and a free-stream dynamic pressure of $q_\infty = 9.5604 \times 10^4 \text{ Pa}$ (2000 psf) as used in the previous work by Rodi.^{1,5} The wall of the leading edge is specified with a constant wall temperature ($T_w = 311.11 \text{ K}$), and the no slip condition for velocity. All outlet boundaries are specified with a zero-

gradient boundary condition for all properties. This treatment is suitable as long as the flow is supersonic at the boundary.³ The field is initialized with a zero velocity field at the free-stream static pressure and static temperature. The steady state solution of the flow-field is then achieved by marching forward in time until changes in the properties of the flow field are negligible.

D. Thermophysical Properties

In order to account for the large temperature changes in the simulation, the fluid's thermodynamic properties are modelled. The gas specific heats are modelled using a 7-coefficient NASA polynomial for JANAF thermophysical data.¹⁵ The polynomials are given in Equations 4 to 6.

$$c_p = R_g(a_1 + a_2T + a_3T^2 + a_4T^3 + a_5T^4) \quad (4)$$

$$H = R_gT(a_1T + a_2T^2/2 + a_3T^3/3 + a_4T^4/4 + a_5T^5/5 + a_6) \quad (5)$$

$$S = R_g(a_1 \ln T + a_2T + a_3T^2/2 + a_4T^3/3 + a_5T^4/4 + a_7) \quad (6)$$

The viscosity is modelled using Sutherland's law^{3,16} shown in Equation 7.

$$\mu = \mu_o \frac{T_o + C}{T + C} \left(\frac{T}{T_o} \right)^{3/2} \quad (7)$$

The thermal conductivity can also be modelled using Sutherland's law, but for these calculations it is modelled using the modified Eucken Method given in Equation 8.

$$\kappa = \mu c_v \left(1.32 + \frac{1.77R_g}{c_v} \right) \quad (8)$$

III. Comparison of Flow-field Predictions

Analysis has been performed at the properties described in Section C.2 for a selected arbitrary test geometry. Figure 4 shows Mach number isolines for the geometry shown in Figure 1. The geometry was intentionally selected to test the accuracy of the HyPE2D flow simulation and the Newton-Kays model compared to rhoCentralFoam. This geometry is an appropriate test case due to its relatively high curvature corners, and low curvature in the vicinity of the stagnation point. We can see that both results show good qualitative agreement, with little noticeable difference between the two flow-fields.

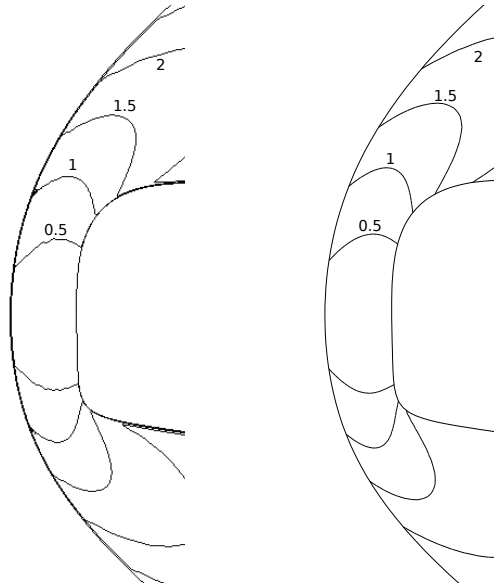


Figure 4. Mach number iso-lines using rhoCentralFoam (Left) HyPE2D (Right)

The predicted laminar heat flux for the BCLE has been compared in Figure 5 for the three different analysis techniques described in Section II. The quality of the results found from HyPE2D is evident due to the close agreement with OpenFOAM. The locations of the peaks in wall heat flux distribution coincide closely and the magnitudes are only marginally over-predicted. A major deficiency of the Newton-Kays model (Section A) is seen at the regions with either significantly high curvature or low curvature. The curvature is low close to the stagnation point and this results in a significant under-prediction of the local wall heat flux. Around the corners where the curvature is high, the heat transfer is over-predicted. However, the Newton-Kays model correctly approximates the qualitative response to changes in local curvature and pressure gradient. A major deficiency of both HyPE2D and the Newton-Kays model is the poor performance close to the stagnation point. In order to obtain smooth data in this region using HyPE2D, a very fine discretization in the stream-wise direction is required. Therefore in both of these methods, the region very close to the stagnation point ($\pm 5^\circ$) is interpolated through from points outside this region, yielding smooth results.

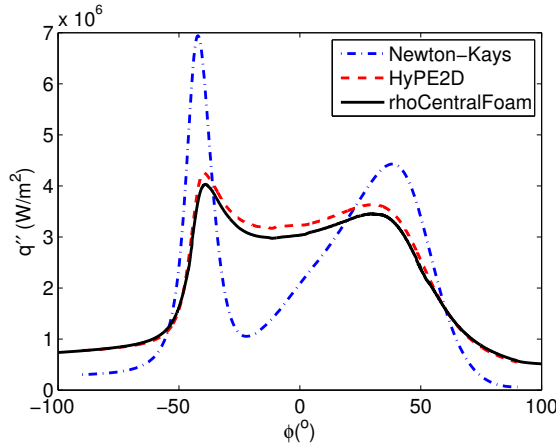


Figure 5. Comparison of predicted wall heat flux (W/m^2) distribution

Predictions for pressure distribution along the BCLE surface are compared in Figure 6. The surface pressure distribution is important for the prediction of drag, as well as the effect of the shape on the stability of the laminar boundary layer. The predicted pressure distributions show reasonable qualitative agreement between all three analysis methods. However, the predicted gradients in pressure around the sharp corners are exaggerated by the modified Newton's method. A deficiency of the Newton-Kays model is its ability to predict the post-shock stagnation pressure. The value of $C_{p,max}$ is calculated using frozen gas properties (constant specific heats) which affects the post-shock properties. While the value of $C_{p,max}$ could be corrected by performing an equilibrium shock calculation, the primary deficiency of the method is with the modified Newton's method itself, not the specific value of $C_{p,max}$. The predicted pressure distributions from HyPE2D and rhoCentralFoam match closely. This agreement indicates that for these flow conditions, the assumption that the boundary layer does not significantly impact the inviscid flow is valid. Additionally, the adequate accuracy of the numerical solution to the equilibrium jump equations is indicated by the closely matching stagnation point pressure.

The comparison of the predictive methods raises important questions about the applicability of the Newton-Kays model for a shape optimization routine. In the present study, and in previous work,^{1,5} Bezier curves were utilized because of their increased flexibility, and because they generate continuous geometries with continuous derivatives. However, a more robust physics model is required in order to accurately account for increased geometric complexity. For example, the Bezier curve approach allows for geometries that incorporate local regions of high and low curvature. We have seen here that the modified Newton's method, when coupled with Kays laminar heating, results in decreased accuracy in both of these cases. Thus, it is possible that when an optimization objective function requires evaluation of either a low or high curvature geometry, the optimized result will be unsatisfactory using the Newton-Kays model. For such a case, attention should be paid to limiting the design space to ensure accuracy. Additionally, an important consideration when using Newton-Kays model is the quality of the analysis itself. For example, in the best case, the Newton-Kays model may arrive at the same optimized geometry as a more sophisticated analysis. However, a designer

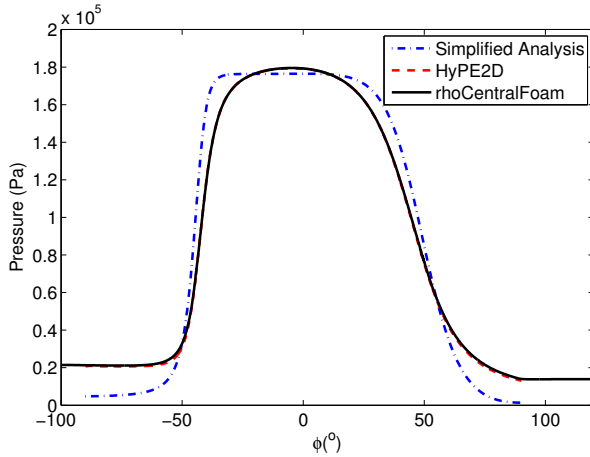


Figure 6. Comparison of predicted pressure (Pa) distribution

must then check the result in order to avoid over-predicting any performance benefits of the new geometry, or failing to predict changes in flow-field topology such as boundary layer separation or turbulent transition. Some of these points are discussed in Section IV using the current optimization results.

IV. Optimization Results

A. Peak Heat Flux Minimization Using Newton-Kays Model

Optimizations were performed to achieve a minimum peak wall heat flux on the leading edge of an 8 degree wedge. The leading edge geometries are generated by changing the location of 4 Bezier curve control points. The genetic algorithm in Matlab's Optimization Toolbox¹⁷ was used in this work. In order to keep the geometries physically realistic, a penalty function was used to limit the resulting geometries to have a similar cross-sectional area for a Hemi-Cylindrical Leading Edge (HCLE). The objective function for geometries with a cross-sectional area beyond $\pm 1\%$ of that of a HCLE were penalized. This penalty function was also used by Rodi in his optimization study.⁵ Optimizations were first performed using the Newton-Kays model. A major benefit of this technique is the low computational cost. Consequently, large sample populations can be evaluated for many generations to ensure a highly resolved optimal result. The optimizations were performed using a population of 3000 and were run until a convergence of 10^{-10} in the objective function was reached. The results typically converged in less than 400 generations. Optimizations were repeated to ensure that the results were correct and not dependent on the choice for the initial population. The non-linear and asymmetrical nature of the problem leads to two possible optimized geometries. One solution involves a reduced radius of curvature corner at the upper surface, and the other involves a reduced radius of curvature corner at the lower surface. The two optimized results are shown in Figure 7. The two geometries result in nearly the same peak convective heat flux with only a 0.2% difference. The optimal result with the sharp corner at the upper surface is similar to the geometry found in the previous work performed by Rodi⁵ using particle swarm optimization and is therefore the focus of the proceeding analysis.

B. Peak Heat Flux Minimization Using HyPE2D

HyPE2D offers a significant advantage over full Navier-Stokes simulations in terms of the required computational resources. However, the cost associated with HyPE2D is still much higher than simplified analysis techniques. In order to reduce the time required for the HyPE2D optimizations, the design space was limited to a $\pm 5\%$ region of the design space for each control point encapsulating the optimized result from the optimization using the Newton-Kays model. Additionally, this ensured that the improved optimization was working in the design space close to the previous optimized result. The size of the reduced design space region was chosen arbitrarily and then checked to ensure that the correct peak heat flux minima was in fact located within the design space. Due to difficulties in visualizing the design space in these dimensions, random geometries within the design space were generated and the limits of the space were found in the X-Y

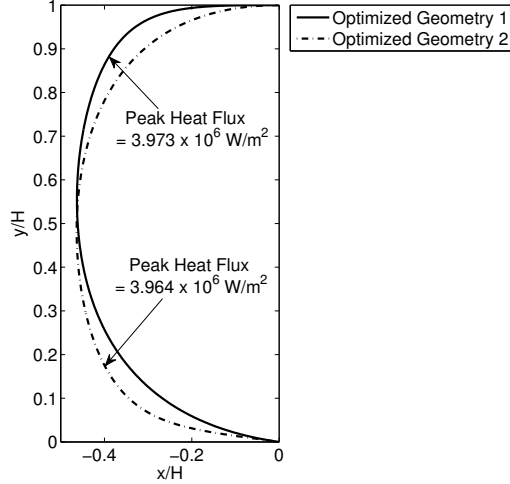


Figure 7. Optimized geometries using the Newton-Kays model

plane, and for curvature. The limits of the design space for the HyPE2D optimization are shown in Figure 8. The flexibility of the design space when using Bezier curves is clear from 8. By reducing the design space, the optimization was limited to varying the radial dimension close to the stagnation point, and the radius of curvature at the upper surface. The optimization using the HyPE2D flow model was performed using a population of 102 (run in parallel on a 6 processor CPU), and was run until the mean change in the fitness function was less than 1%. A converged result was achieved after 100 generations (10302 unique HyPE2D flow simulations). A typical convergence for the HyPE2D optimizations performed is shown in Figure 9.

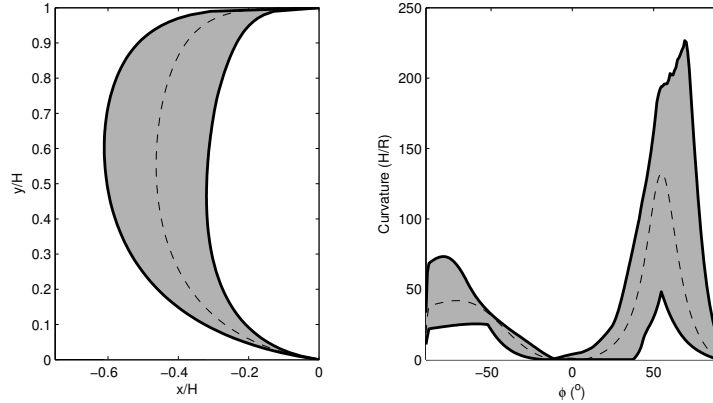


Figure 8. Design space limits for HyPE2D optimization (dashed line corresponds to optimized shape)

The optimized geometries using the Newton-Kays model and HyPE2D are shown in Figure 10. The improved flow model changes the optimal geometry slightly. A smaller radius of curvature is found at the top, while a larger radius of curvature is found in the vicinity of the stagnation point. Table 1 shows the performance of the two optimized geometries compared to the HCLE. All of the analysis methods show a significant decrease in peak heat flux compared to the HCLE. Both optimization methods have resulted in a leading edge that performs significantly better than the HCLE. However, the shape found using HyPE2D performs slightly better. As is expected the Newton-Kays model predicts a greater decrease in peak convective heat flux for the optimized geometry found using the same method. The predicted heat flux profiles along the leading edge surface are shown in Figure 11. These profiles show that the different result is due to the Newton-Kays model's over-prediction of convective heat flux in regions of high curvature. This over-prediction means that a more conservative shape is selected when in fact, a higher curvature can be

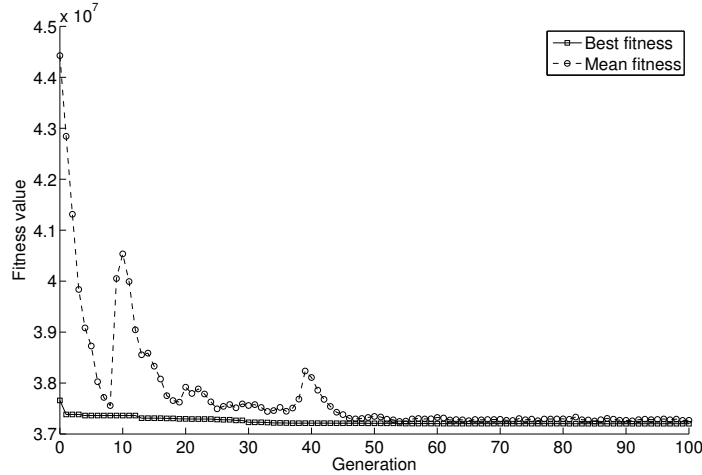


Figure 9. Optimization convergence for genetic algorithm with HyPE2D

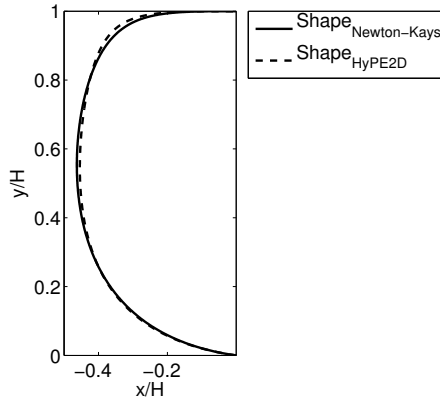


Figure 10. Optimal leading edge geometries found by various methods

tolerated.

Table 1. Percent decrease in peak heat flux compared to hemi-cylindrical leading edge

	Newton-Kays	HyPE2D	rhoCentralFoam
Shape _{Newton-Kays}	19.4%	13.6%	15.6%
Shape _{HyPE2D}	14.1%	16.5%	17.7%

Another important consideration in these optimizations is the increase in drag as a result of the decreased peak convective heat flux. The pressure drag coefficient was calculated for each geometry using the pressure calculated by rhoCentralFoam. The HyPE2D optimized shape resulted in a pressure drag increase of 8.67%, and the Newton-Kays model optimized shape resulted in an increase of 6.66%. The present study only optimized for minimum peak heat flux, and thus the drag cost was not accounted for. Future analysis could include a multi-objective optimization for the reduction of both drag and heat flux.

C. Sensitivity of Peak Heating to Displacement and Curvature

In order to examine the relative performance compared to geometries close within the design space, an analysis was performed using random generation of geometries within a significantly reduced design space. The geometries were created by randomly relocating the Bezier curve control points within the design space. Here, approximately 5×10^5 geometries were created and then filtered to only include those within $\pm 1\%$

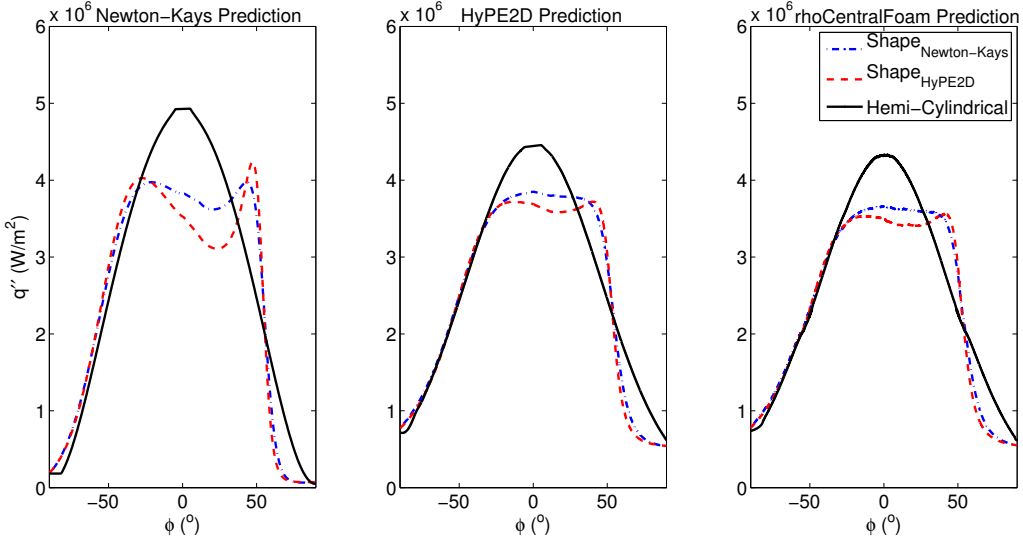


Figure 11. Heat transfer predictions for the optimized results in Figure 10

of the cross-section area of the geometry. This is to ensure consistency between the current method and the genetic algorithm fitness function. After filtering, approximately 36000 geometries that met the area requirement were evaluated and compared against the optimal geometry from Section IV. The random geometries were binned based on their maximum percent difference in radial dimension. Because of the large number of calculations performed in this brute force method, the Newton-Kays model was used for the performance evaluation. In each bin, the mean, maximum and minimum percentage change in peak heat flux was calculated. The results are shown in Figure 12. It is clear from the results that the optimization has performed well. A small change in the radial dimension results in a significant increase in peak convective heat flux. For example, a 2%-3% uncertainty in the leading edge geometry would result in, at minimum, a 3% increase in peak heat flux. However, it could result in up to a 14% increase, and on average would result in a 7% increase. The relationship between surface geometry imperfections and a heat flux penalty could provide the means for a vehicle designer to account for factors such as fabrication tolerances when designing leading edges. For example, in the worst case, a machine tolerance of 10/1000 of an inch in the fabrication of a 1 inch radius leading edge could result in a 5% penalty in the peak heat flux.

V. Conclusion

A simplified model (modified Newton's method with Kays laminar heating) and a new reduced-order model (HyPE2D) were used to optimize the two-dimensional leading edge geometry at Mach 10 based on a peak laminar heat flux. The performance of each model was assessed based on comparisons to fully compressible two-dimensional Navier Stokes simulations using OpenFOAM's rhoCentralFoam solver. HyPE2D showed excellent agreement with the rhoCentralFoam results for both pressure and convective heat flux distributions. However, HyPED2D required the use of the simplified model to initially reduce the size of the design space such that the HyPE2D optimization could complete in a practical amount of time. The simplified model, on its own, failed to accurately predict the surface heat flux in areas of high or low radius of curvature. Despite this deficiency, both models produced a very similar optimized shape. The heat flux of each optimized shape was compared to that of a hemi-cylindrical leading edge geometry using OpenFOAM. The optimized geometry obtained from the simplified model resulted in a 15.5% decrease in peak heat flux and a 6.7% increase in pressure drag. The optimized geometry using HyPE2D resulted in a 17.7% decrease in peak heat flux and a 8.67% increase in pressure drag. Analysis of the design space around the optimal geometry was performed to quantify the sensitivities between small changes in geometry and the associated heat flux penalty. It was found that a significant heat flux penalty ($\approx 5\%$) can occur, even for very small deviations in the leading edge radius ($< 1\%$).

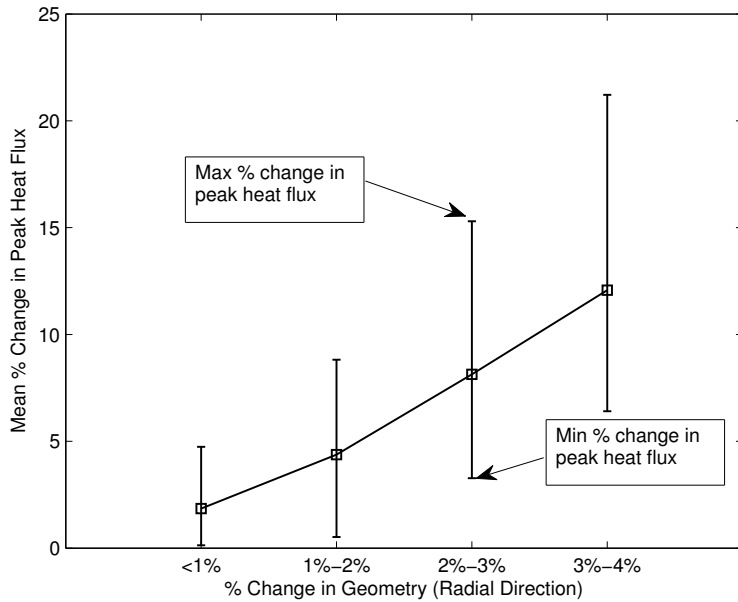


Figure 12. Relative performance of geometries close within the design space

Acknowledgments

This research was enabled in part by support provided by WestGrid (www.westgrid.ca) and Compute Canada Calcul Canada (www.computecanada.ca). Financial support was provided by the Natural Sciences and Engineering Research Council of Canada (NSERC).

References

- ¹Rodi, P., "Optimization of Bezier Curves for High Speed Leading Edge Geometries," *51st AIAA Aerospace Sciences Meeting including the New Horizons Forum and Aerospace Exposition*, American Institute of Aeronautics and Astronautics, Grapevine (Dallas/Ft. Worth Region), Texas, Jan. 2013.
- ²Cui, K. and Hu, S.-C., "Shape Design to Minimize the Peak Heat-Flux of Blunt Leading-Edge," *51st AIAA Aerospace Sciences Meeting*, No. January, American Institute of Aeronautics and Astronautics, Grapevine (Dallas/Ft. Worth Region), Texas, 2013, pp. 1–14.
- ³Anderson, J. D., *Hypersonic and High-Temperature Gas Dynamics*, American Institute of Aeronautics and Astronautics, Blacksburg, Virginia, 2nd ed., 2006.
- ⁴O'Brien, T. F. and Lewis, M. J., "Power Law Shapes for Leading-Edge Blunting with Minimal Shock Standoff," *Journal of Spacecraft and Rockets*, Vol. 36, No. 5, Sept. 1999, pp. 653–658.
- ⁵Rodi, P. E., "Integration of Optimized Leading Edge Geometries Onto Waveride Configurations," *53rd AIAA Aerospace Sciences Meeting*, No. January, American Institute of Aeronautics and Astronautics, Kissimmee, Florida, 2015, pp. 1–21.
- ⁶Kays, W., Crawford, M., and Weigand, B., *Convective Heat and Mass Transfer*, McGraw-Hill, New York, NY, 4th ed., 2005.
- ⁷Salas, M. D., *A Shock-Fitting Primer*, Taylor & Francis Group, LLC, Bova Raton, FL, 2010.
- ⁸Schetz, J. A., *Boundary Layer Analysis*, Prentice Hall, Upper Saddle River, New Jersey, 1st ed., 1993.
- ⁹Hinman, W. S., Johansen, C. T., and Wilson, S. J., "Application of Simplified Numerical and Analytical Methods for Rapid Analysis in Atmospheric Entry Vehicle Design," *53rd AIAA Aerospace Sciences Meeting*, No. January, Kissimmee, Florida, 2015, pp. 1–14.
- ¹⁰Cohen, C. and Reshotko, E., "Similar solutions for the compressible laminar boundary layer with heat transfer and pressure gradient (Rept. 1293)," Tech. rep., N.A.C.A., 1956.
- ¹¹*OpenFOAM*, OpenCFD Ltd., 2015.
- ¹²Greenshields, C. J., Weller, H. G., Gasparini, L., and Reese, J. M., "Implementation of semi-discrete, non-staggered central schemes in a colocated, polyhedral, finite volume framework, for high-speed viscous flows," *International Journal for Numerical Methods in Fluids*, 2009, pp. n/a–n/a.
- ¹³Arisman, C., Johansen, C. T., Galuppo, W., and McPhail, A., "Nitric Oxide Chemistry Effects in Hypersonic Boundary Layers," *43rd Fluid Dynamics Conference*, American Institute of Aeronautics and Astronautics, Reston, Virginia, June 2013.
- ¹⁴Hinman, W. S. and Johansen, C. T., "Numerical Investigation of Laminar Near Wake Separation on Circular Cylinders

at Supersonic Velocities," *29th Congress of the International Council of the Aeronautical Sciences*, International Council of the Aeronautical Sciences, St. Petersburg, Russia, 2014, pp. 1–10.

¹⁵NIST-JANAF, "NIST-JANAF Thermochemical Tables," 2013.

¹⁶Rathakrishnan, E., *Theoretical Aerodynamics*, John Wiley & Sons Singapore Pte. Ltd., Singapore, 1st ed., 2013.

¹⁷Matlab R2014a Optimization Toolbox, The Mathworks Inc., Natick, Massachusetts, United States, 2014.